MOCVD of rhodium, palladium and platinum complexes on fluidized divided substrates: Novel process for one-step preparation of noble-metal catalysts

Jean-Cyrille Hierso,[1] Philippe Serp,[1] Roselyne Feurer[2] and Philippe Kalck[1]*
[1]Laboratoire de Catalyse et Chimie Fine, Ecole Nationale Supérieure de Chimie de Toulouse, 118 route de Narbonne, 31077, Toulouse Cédex, France
[2]Laboratoire de Cristallochimie, Réactivité et Protection des Matériaux, (UPRESA–CNRS 5071), Ecole Nationale Supérieure de Chimie de Toulouse, 118 route de Narbonne, 31077, Toulouse Cédex, France

A new one-step method, entitled fluidized-bed metal-organic chemical vapor deposition (FBMOCVD) of preparing highly dispersed metal-supported catalysts is reported. The following complexes were studied and used as CVD precursors in presence of H_2: $[Rh(\mu\text{-}Cl)(CO)_2]_2$, $Rh(allyl)_3$, $Rh(acac)(CO)_2$, $Pd(allyl)(hfac)$, $Pd(allyl)(Cp)$, $Pt(COD)(CH_3)_2$. (acac, acetylacetonato; hfac, hexafluoroacetylacetonato; Cp, cyclopentadienyl; COD, cyclooctadienyl). In a first approach, depositions on planar substrates were carried out to establish the best experimental conditions to obtain good-quality deposits. X-ray diffraction, X-ray photo-electron spectroscopy and electron microprobe studies were realized on the resulting thin films. Analyses of the products contained in the gas phase after and during deposition were performed by mass spectrometry and GC–MS. Finally, catalysts prepared by FBMOCVD were characterized by transmission electron microscopy–energy dispersion spectroscopy (TEM–EDS), metal-loading determinations and specific-surface measurements (BET). Dispersed nanosized aggregates were obtained, showing high activities in alkene hydrogenation and alcohol hydrocarbonylation. © **1998 John Wiley & Sons, Ltd.**

Appl. Organometal. Chem. **12**, 161–172 (1998)

*Correspondence to: Philippe Kalck, Laboratoire de Catalyse et Chimie Fine, Ecole Nationale Supérieure de Chimie de Toulouse, 118 route de Narbonne, 31077, Toulouse Cédex, France. E-mail: pkalck@ensct.fr.
Contract/grant sponsor: EEC BRITE–EURAM program.
Contract/grant sponsor: Conseil Scientifique de l'Institut National Polytechnique (BQR Action).
Contract/grant sponsor: Conseil Régional Midi-Pyrénées.
Contract/grant sponsor: Ministère de l'Engeignement Supérieur et de la Recherche.

 CCC 0268–2605/98/030161–12 $17.50

Keywords: chemical vapor deposition; platinum; palladium; rhodium; heterogeneous catalysts; fluidized bed; MOCVD

Received 30 December 1996; accepted 30 March 1997

INTRODUCTION

Catalysts play a major role in our modern industrial and economic structures.[1,2] Indeed, 80% of the petrochemical products and chemicals currently produced by industry have been in contact with a catalyst during at least one step of their elaboration. Both homogeneous and heterogeneous systems offer advantages and drawbacks. The attraction of using heterogeneous catalysts is that they can be separated easily from the reaction products. Furthermore they display generally good mechanical and thermal stabilities, and high activities. This explains why there are numerous industrial processes involving supported catalysts,[3,4] not only in heavy industrial chemistry (NH_3 synthesis, SO_2 oxidation or petrochemistry…) but also in fine chemistry (asymmetric hydrogenation…).

However, due to preparation methods, some drawbacks remain. Typical heterogeneous catalyst preparation methods include co-crystallization,[5,8] ion-exchange[6,8] or impregnation.[7,8] They normally require the use of metal complexes to obtain the active, pure metal dispersed on a metal oxide support such as Al_2O_3, SiO_2 or TiO_2. Various oxidation and reduction steps are necessary: indeed, during the calcination step, oxidation to remove organic or inorganic ligands can also oxidize the supported metal to form the metal oxide.[9] Consequently this step requires a subsequent reduction process to regenerate the active metal form.

The high temperature (>400 °C) required for these steps can cause aggregation of the supported metal particles, resulting in changes in particle size and thus in size-dependent properties such as activity and selectivity.[6,10] Moreover, the microstructure of the oxide support can also be modified, leading to decreases in specific area, or changes in porosity as well as in chemical properties.[11] Finally, high-temperature processes preclude the use of some sensitive supports.[12] For these reasons potential alternative methods must be sought.

The potential of metal-organic chemical vapor deposition (MOCVD) processes for the preparation of noble-metal supported catalysts from suitable precursors has been investigated. The great number of metal-organic and organometallic compounds of platinum group metals allows us, using a convenient reactive gas, to deposit pure metal particles at low temperature (<150 °C). In this paper a new, one-step method entitled fluidized-bed metal-organic chemical vapor deposition (FBMOCVD), which provides easy access to highly dispersed metal-supported catalysts, is reported.

BACKGROUND

Catalytic-metal chemical vapor deposition (CVD)

In 1890, high-purity nickel was deposited by Mond in the first metal-organic chemical vapor deposition process reported. With regard to the platinum group metals, Marboe[13] first described (1947) the deposition of platinum, but it was the work of Rand[14,15] which was the actual starting point of detailed noble-metal CVD studies. The first attempts at noble-metal deposition in the absence of a carrier gas gave films containing important amounts of impurities.[14,15] Girolami and co-workers later reported the synthesis of high-quality palladium and platinum films, still without using a carrier gas, and showed the great importance of choosing the right precursor complexes.[16] At the same time, the groups of Kaesz and Puddephatt described noble-metal deposition using a reactive gas such as dihydrogen or dioxygen.[17,18] As a result, dramatic decreases in the temperature of deposition and high-purity depositions were obtained.

However, despite the excellent results reported concerning thin-films deposits on planar substrates (mainly for electronics applications), relatively few studies on CVD of catalytic materials have been reported. It is noteworthy that recently three groups have described a two-step elaboration of supported catalysts using CVD. Dossi and co-workers have prepared palladium and platinum/zeolite catalysts by adsorption of organometallic complexes from a gaseous phase, the supported materials then being heated in an H_2/He flow at high temperature.[19–21] It was also shown that $Ni(CO)_4$ can be adsorbed on activated carbon in a fluidized bed and then, in a second step, decomposed at 250 °C in a dinitrogen atmosphere.[22] In a similar way, Baerns and co-workers obtained platinum supported on SiO_2, Al_2O_3 or TiO_2 after decomposition of $Pt(acac)_2$ at 300 °C.[23] These processes require prior adsorption of organometallic complexes and do not spare the need for high decomposition temperatures.

CHOICE OF THE PRECURSORS

Several general criteria for selecting CVD precursor complexes are required.[24] Among the various physicochemical properties, good volatility, non-toxicity and thermal stability during the sublimation step are considered essential properties for FBMOCVD. The processing conditions require compounds easily available in good yields, and deposition temperatures below 150 °C.

The following complexes meet the above criteria: $[Rh(\mu\text{-}Cl)(CO)_2]_2$ (**1**), $Rh(allyl)_3$ (**2**), $Rh(acac)(CO)_2$ (**3**), Pd(allyl)(hfac) (**4**), Pd(allyl)(Cp) (**5**) and $Pt(COD)(CH_3)_2$ (**6**) where allyl is η^3-C_3H_5), acac is the acetylacetonato ligand ($CH_3COCHCOCH_3$), hfac is the hexafluoroacetylacetonato ligand ($CF_3COCHCOCF_3$) and Cp is the cyclopentadienyl ligand (η^5-C_5H_5), COD is the cyclo-octadienyl ligand (C_8H_{12}). These compounds are solids at room temperature.

Vapor pressures of the precursor complexes

Control of a given CVD process entails knowledge of the partial pressures of the precursors under the experimental conditions. As these data are still absent from the literature, the dependences of the vapor pressures on temperature for the sublimation of complexes **1–6** were measured. The combined results are shown in Figs. 1 and 2. The heats of sublimation of the precursors obtained from the Clausius–Clapeyron equations associated with these data are displayed in Table 1. Concerning the measured values, it is worth noting the higher

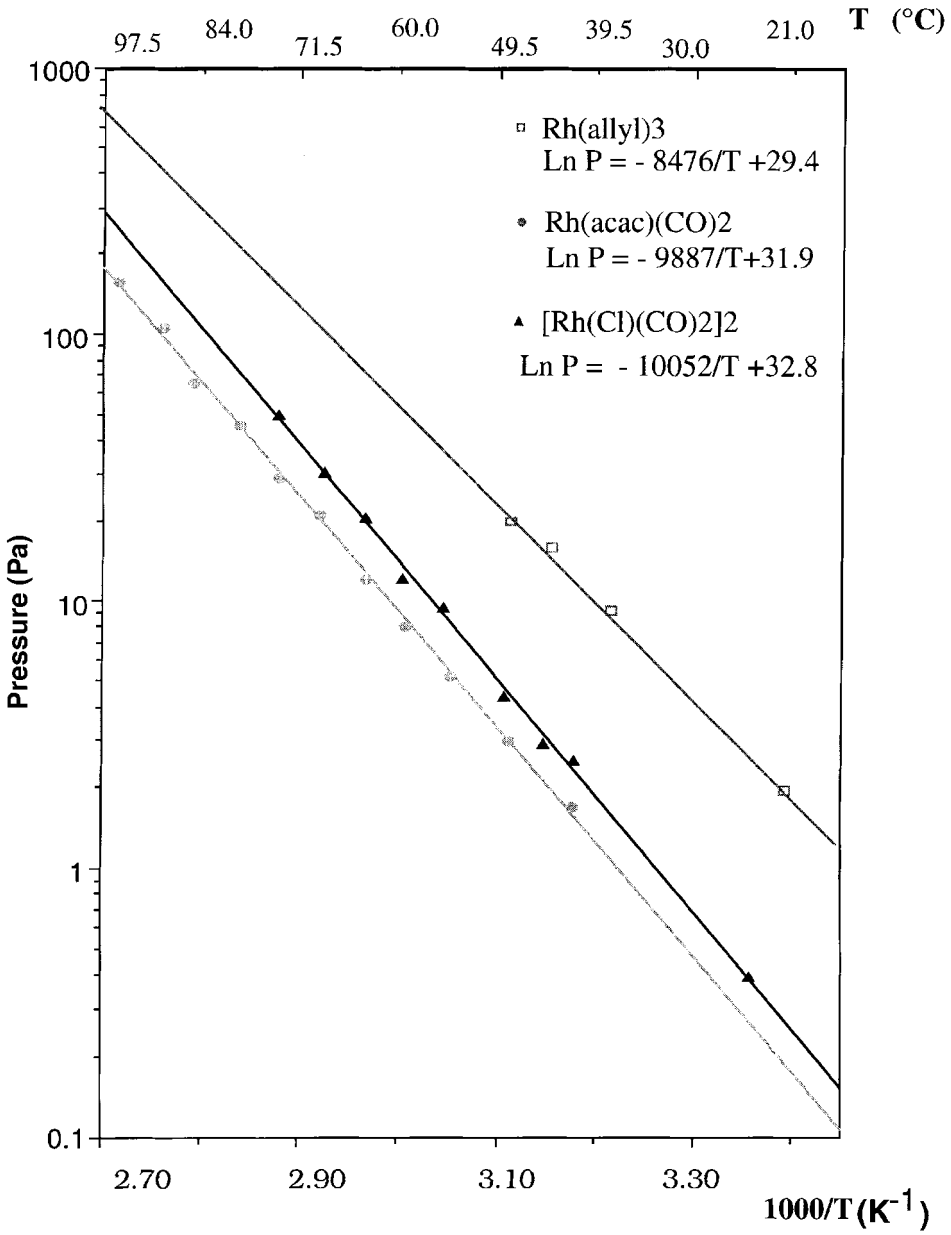

Figure 1 Dependence of the vapor pressures on temperature for **1, 2** and **3**, and the associated Clausius–Clapeyron equations.

vapor pressures of compounds containing allyl ligands.[25]

PROCESSES INVOLVING PLANAR SUBSTRATES

Preliminary investigations on planar substrates were carried out to establish the best experimental conditions to obtain good-quality deposits as catalytic materials, and also to highlight the mechanisms of CVD for selected complexes.

CVD apparatus and physicochemical analyses

Thin-film depositions were realized in a horizontal, hot-wall CVD reactor described elsewhere.[29]

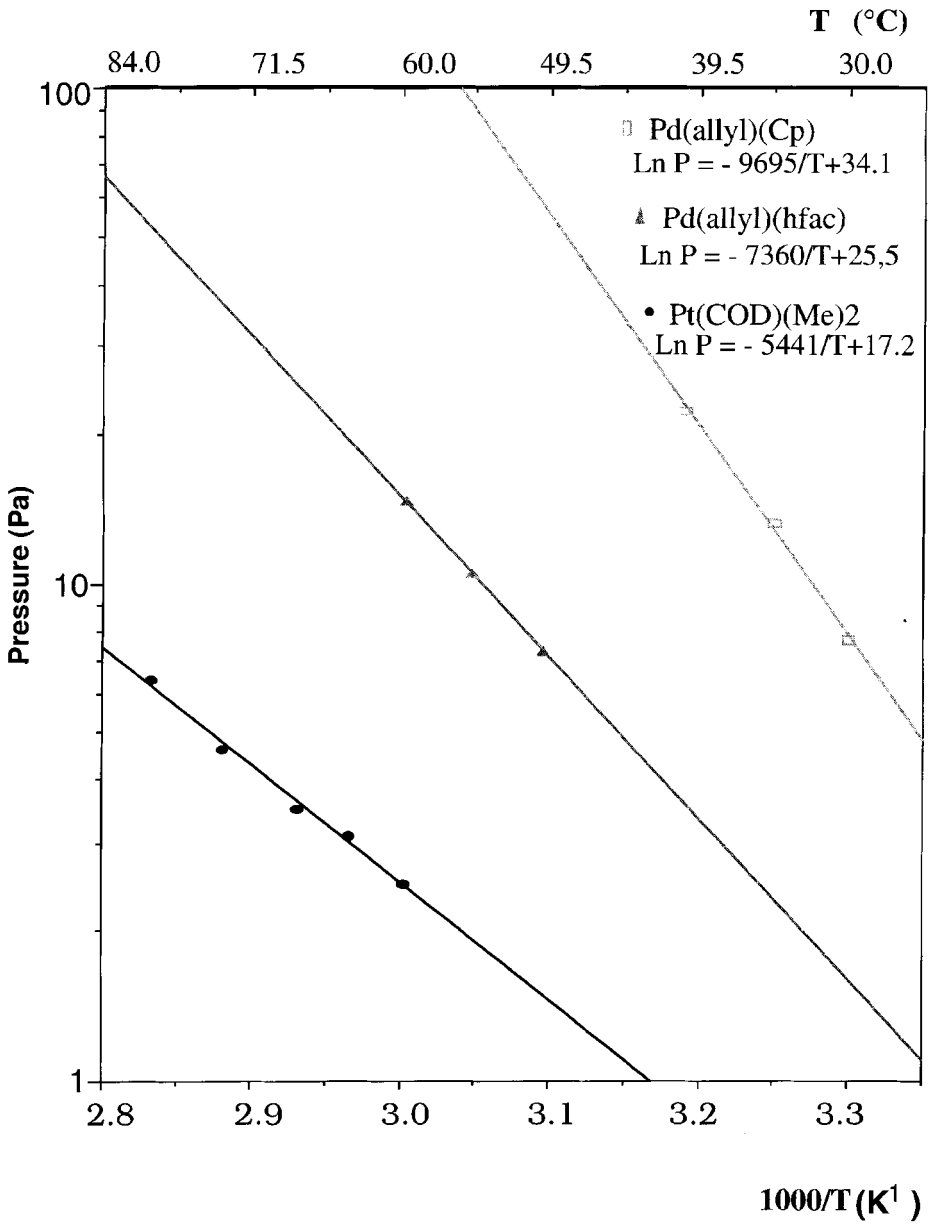

Figure 2 Dependence of the vapor pressures on temperature for **4, 5** and **6**, and the associated Clausius–Clapeyron equations.

Before each deposition, the apparatus was cleaned out with detergent, deionized water and acetone, and then kept for several hours under dynamic vacuum. The glass substrates were boiled in trichloroethane, then in acetone, and finally dried inside the CVD furnace under a helium current and at low pressure.

At the beginning of an experiment, the helium carrier gas was saturated with metal precursor vapors by passing upstream through a sintered glass plate holding the solid metal-organic complex. To fix the vapor pressure, the entire sublimator system was maintained at a constant temperature regulated by a water bath. Dihydrogen was introduced near the substrate to allow better control of the deposition area. The Pyrex tube reactor was heated

Table 1 Heats of sublimation of **1–6**

Metal-organic complex	Heat of sublimation[a] ($kJ\ mol^{-1}$)	Synthesis reference
1	84 ± 3	26
2	70 ± 2	27
3	82 ± 3	28
4	61 ± 3	29
5	81 ± 4	30
6	45 ± 3	31

[a] Error limits are the estimated experimental uncertainties in the measurements.

using a temperature-controlled furnace. An on-line mass spectrometer, Balzers QMS, was set up at the deposition area via a capillary tube. Decomposition gases, as well as unreacted precursor, were trapped at liquid-nitrogen temperature. Liquid residues were analyzed by GC–MS (Perkin-Elmer Q Mass 910). The films were analyzed by X-ray photoelectron spectroscopy (XPS) to identify the surface species. XPS spectra were obtained by using a VG Escalab MK II with an unmonochromatized MgKα X-ray source ($\lambda = 0.989$ nm) at a pressure of 6×10^{-11} kPa. Electron microprobe qualitative and quantitative analyses were realized using a Cameca SX50 electron microprobe. The measurements were carried out in various regions of the samples by comparison with a metal standard (99.9% purity) to obtain volumetric analyses of the films. X-ray diffraction analyses were carried on a Seifert XRD 3000 with CuKα radiation ($\lambda = 0.15406$ nm). Scanning electron microscopy studies were run on a JEOL 6400 apparatus.

Deposition conditions and characterization of deposits

Several different parameters were examined with a view to determining the best experimental conditions for deposition. The results reported here focus on experiments conducted under H_2/He atmospheres. Indeed, the H_2/He mixture led to deposits of improved purity, obtained at lower temperatures, in agreement with our purpose. Physicochemical characterizations were performed on planar substrate deposits by classical surface analysis methods. A very accurate correlation between the present experiments on planar substrates and those in a fluidized bed (*vide infra*) was verified.

Table 2 displays the reaction conditions leading to the highest material purities. A total pressure ranging between 50 and 100 Torr allowed an appropriate molar ratio of precursor, and was consistent with the bubbling fluidization regime of the catalytic supports required by the fluidized-bed process. The molar ratios of the various precursors given in Table 2 were fixed through the total pressure and the sublimator temperature. The amounts of dihydrogen required to remove the ligands, but precluding complete decomposition in the gas phase, vary dramatically with the nature of the starting complex. For instance, the two palladium complexes investigated here are very reactive towards dihydrogen. Therefore only relatively low dihydrogen/carrier gas ratios (8–10%) were necessary during deposition. In all cases, deposits were obtained at temperatures below 100 °C, palladium films of high purity being obtained at unexpectedly low temperatures (35–60 °C).[29]

Scanning electron microscopy of deposits prepared under the conditions displayed in Table 2 shows that rhodium, palladium and platinum films were formed with grain sizes between 100 and 1000 nm.[29] X-ray diffraction studies revealed in all cases the characteristic spectra of the crystalline metals. No particular orientation was observed.

Table 2 Selected experimental conditions for the deposition of **1–6**

Metal-organic complex	Sublimator temperature (°C)	Deposition temperature (°C)	Precursor molar ratio	H_2 molar ratio	Total Pressure (Torr)	Impurities (wt%)
$[Rh(\mu\text{-}Cl)(CO)_2]_2$	50	75	4.2×10^{-4}	2.5×10^{-1}	100	1.5% Cl[a]
$Rh(allyl)_3$	40	60	7.8×10^{-4}	4×10^{-2}	100	7% C[a]
$Rh(acac)(CO)_2$	60	85	7.0×10^{-4}	2.5×10^{-1}	100	14% C[a]
Pd(allyl)(hfac)	40	45–60	1.12×10^{-3}	1×10^{-2}	50	<1% C[b]
Pd(allyl)(Cp)	30	35–60	1.20×10^{-3}	1×10^{-2}	50	<3% C[b]
$Pt(COD)(CH_3)_2$	70	90–120	3.2×10^{-4}	1.0×10^{-1}	90	<1% C[a,b]

[a] XPS analysis from thin-film deposits on SiO_2 planar substrates.
[b] Electron microprobe analysis from thin-film deposits on SiO_2 planar substrates.

Gas-phase studies

In order to gain an insight into the decomposition mechanisms, analyses of the products contained in the gas phase were performed. The inorganic and organic residues were trapped after the reactor, and analysed by GC–MS. More information was gained from on-line mass-spectrometric analyses, by following the gas-phase composition. During various deposition experiments, the evolution of several characteristic fragments was monitored carefully (as described later for **4**). In addition, infrared measurements were used to identify and follow the appearance in the gas phase of certain fragments such as CO or HCl.

Rhodium complexes

Under an inert helium atmosphere, $[Rh(\mu\text{-}Cl)(CO)_2]_2$ produces carbon monoxide above 125 °C and a solid characterized by a Rh/Cl ratio near 1:1. However, when dihydrogen is added to the helium (about 20%, v/v), the loss of CO above 75 °C is detected rapidly by infrared, followed by the formation of HCl in the gas phase. It was shown that in the gas phase, reactive rhodiumhydride species are formed resulting from the loss of CO and HCl from complex **1**.[32] These species presumably interact with particular sites on the support, giving rise to rhodium anchoring. Dihydrogen plays a major role in dechlorination of complex **1** during deposition and thus increases the purity of the deposits.

Decomposition of $Rh(allyl)_3$ leads respectively to propene and 1,5-hexadiene under pure helium and propene/propane mixtures under an H_2/He atmosphere, as determined by both infrared and mass spectrometry. Under helium the decomposition of $Rh(acac)(CO)_2$ gives rise to CO, CO_2, acetone and butanone. This latter complex heated under H_2/He (85 °C) decomposes first with loss of CO, then by formation of 2,4-pentanedione.[26]

Palladium complexes

Thermolysis of the Pd(allyl)(Cp) precursor in the absence of any reactive gas was reported to give a mixture of propene, cyclopentadiene and traces of hexadiene. This behavior was interpreted as resulting predominantly from a radical mechanism.[16] Under our conditions, introduction of dihydrogen produces cyclopentene, cyclopentane, propane and presumably propene; these results are more consistent with concerted mechanisms involving hydrogenation of the original ligands and their clean elimination. The relative concentrations of the various resulting organic compounds correlate with the amounts of dihydrogen present in the medium.[29]

Concerning the gas-phase products resulting from Pd(allyl)(hfac), as previously detected for Pd(allyl)(Cp), the allyl ligand is mainly hydrogenated to propene and propane. For instance, on-line mass spectrometry measurements during a deposition experiment are displayed in Fig. 3. The variations in the amounts of propane and propene are shown through the evolution of their two major fragments in the gas phase. It clearly appears that when dihydrogen is cut off during an experiment, hydrogenation still continues for several minutes by means of chemisorbed dihydrogen on the surface of the palladium deposit. The relative amounts of propane decrease regularly, whereas during the same time the amounts of propene increase, demonstrating that as the H_2 partial pressure diminishes the first step of hydrogenation is favored, i.e. the formation of propene rather than propane. As expected, switching the dihydrogen flow on rapidly restores the initial rates.

However, with the Pd(allyl)(hfac) complex the hfac ligand follows a different pathway. Whereas a negligible part of the acetylacetonato ligand is hydrogenated, a major part decomposes into trifluoropropanone and various unidentified organofluorine compounds.

Platinum complex

More recently, we examined the decomposition of $Pt(COD)(CH_3)_2$. Under helium, this compound decomposes at 90 Torr above 240 °C giving rise to cyclo-octadiene (GC–MS) and methane (observed exclusively by on-line MS experiments). These products were reported to form under a dinitrogen atmosphere (FTIR).[33] Under these conditions, significant amounts of graphitic carbon were incorporated in the deposits. Introducing a partial pressure of dihydrogen in the carrier gas leads to decomposition of **6** beginning around 90 °C, and providing mainly cyclo-octane, cyclo-octene, traces of cyclo-octadiene (GC–MS) and methane (on-line MS). The incorporation of carbon into the platinum deposits was noticeably reduced (Table 2).

Interpretation of results

GC/MS characterization of trapped residues, confirmed by on-line mass spectrometry analyses during the deposition process, is summarized in Table 3. We observe that, *mutatis mutandis* for each complex, hydrogen assists the removal of certain

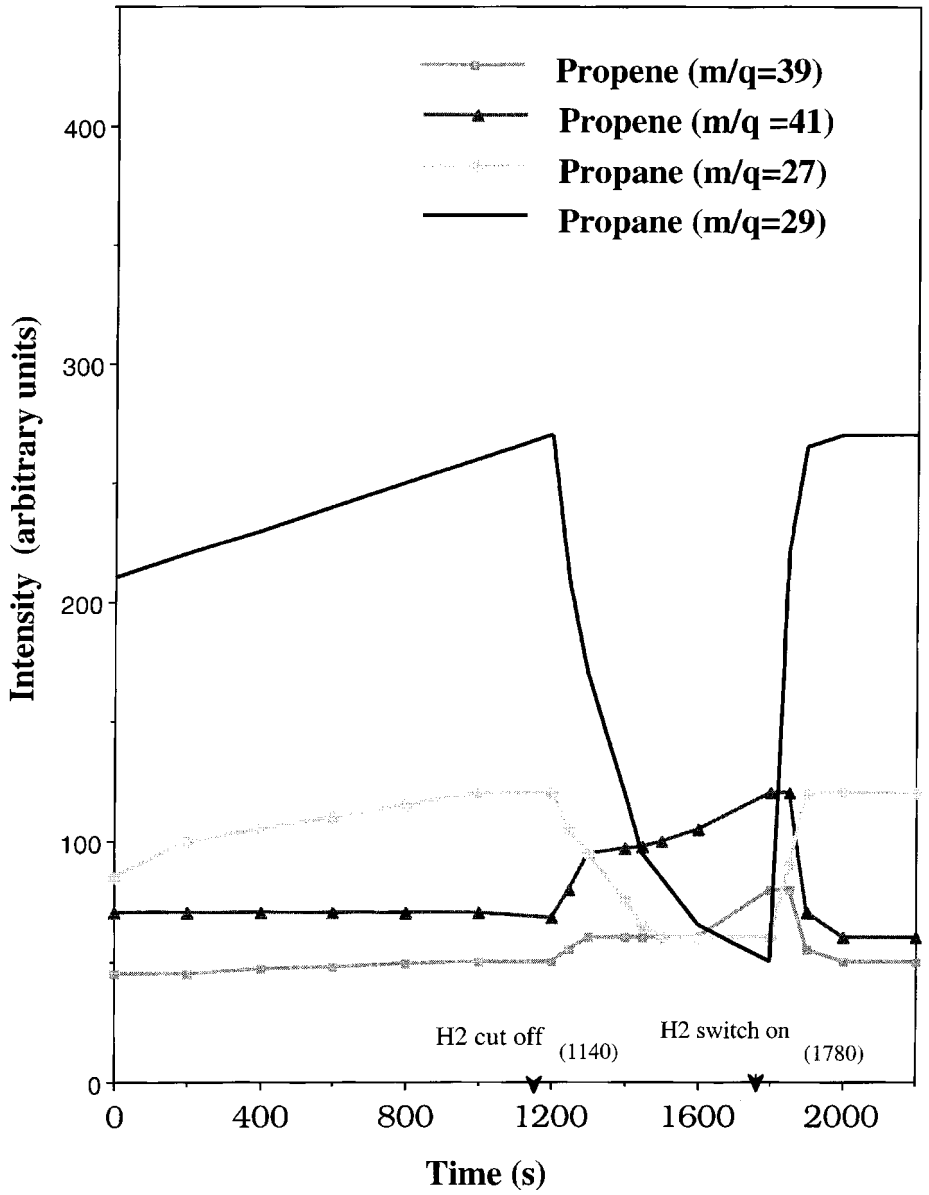

Figure 3 Propane and propene evolution in the gas phase during Pd(allyl)(hfac) deposition in an H_2/He mixture (1 vol%). The substrate temperature was 60 °C. Dihydrogen flow was cut off after 1140 s, and switched on after 1780 s, as indicated by arrowheads on the abscissa.

ligands as stable volatile species, giving for example HCl or saturated hydrocarbons such as propane or methane. Concerning organic ligands removed in the absence of dihydrogen, some stable fragments are lost, e.g. methane from **6** or propene from **2** and **5**. Consequently, in these cases the hydrogenation of the ligand can only be due to cleavage of H–C bonds in some ligands, leading to unsaturated reactive fragments, which could then explain the presence of unwanted carbon in the deposits prepared in the absence of dihydrogen.

Analyses of films deposited on planar substrates, and of species in the gas phase during the deposition process, led us to determine a range of

Table 3 Identification of the decomposition products from deposits under an H_2/He mixture

Metal-organic complex	Gaseous decomposition products
$[Rh(\mu\text{-}Cl)\ (CO)_2]_2$	HCl + CO
$Rh(allyl)_3$	Propene (C_3H_6) + propane (C_3H_8)
$Rh(acac)(CO)_2$	CO + 2,4-pentanedione (acacH)[a]
Pd(allyl)(hfac)	Propene (C_3H_6) + propane (C_3H_8) + trifluoropropanone (CF_3COCH_3) + unidentified organofluoride products + hexafluoro-2,4-pentanedione (hfacH)[a]
Pd(allyl)(Cp)	Propane (C_3H_8) + propene (C_3H_6) + cyclopentane (C_5H_{10}) + cyclopentene (C_5H_8) + cyclopentadiene (C_5H_6)[a]
$Pt(COD)(CH_3)_2$	Methane (CH_4) + cyclo-octane (C_8H_{16}) + cyclo-octene (C_8H_{14}) + cyclo-octadiene (C_8H_{12})[a]

[a] Trace amounts detected.

parameters for a clean CVD reaction. The transposition of this process to porous divided supports requires adaptation, to some extent, of the previous parameters, and also development of some new ones.

FLUIDIZED-BED PROCESSES

Our aim is to prepare highly dispersed catalytic materials, i.e. nanosized metal particles (1–5 nm) supported on porous carrier with a specific area at least of 150 $m^2\ g^{-1}$, the metal leading being 0.3–5 wt%. To have the maximum number of metal atoms offered to the reactants, the dispersion (ratio of metal accessible to metal introduced) should be as high as possible (typically >60%).

It appears that a fluidized bed should offer convenient processing conditions to obtain a statistical distribution of small metallic aggregates on the whole surface of the support grains. Heterogeneous catalyst preparation involves handling supports with high specific areas. These increased areas are characterized by surface inhomogeneities compared with planar substrates, including specific sites where aggregate nucleation can occur. To obtain highly dispersed metallic particles, it is necessary to favor particle nucleation as opposed to particle growth of the aggregates. The low temperatures and the high surface area for gas/solid interactions are favorable for achieving these requirements. The total flow rate needs to be adapted to each solid, particularly to its minimal fluidization rate which is in a narrow relationship between density and grain size.[34] Low-pressure areas were determined to adjust (or maintain simultaneously) the correct molar ratio of precursor in the gas phase and a bubbling regime for the fluidized bed. In addition to the correct sizes of the particles and their homogeneous repartition, the method of preparing supported catalysts is considered proper if the specific area of the starting material is not decreased, mainly because the micropores must not be clogged.

The whole apparatus designed to prepare metal-supported catalysts is shown in Fig. 4. Various metals (rhodium, platinum, palladium) and supports [SiO_2, Al_2O_3, activated carbon (C*)] have been used. At the beginning of a general procedure,

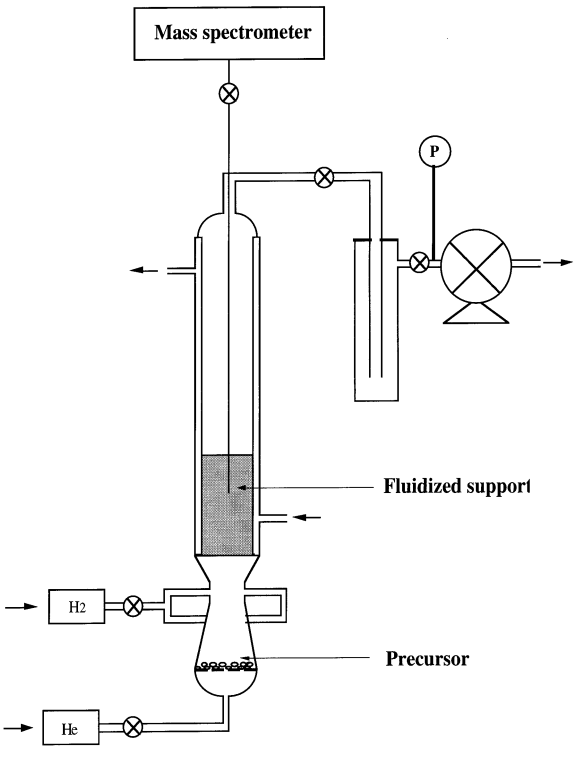

Figure 4 Schematic diagram of the fluidized-bed CVD reactor.

Table 4 Example of experimental conditions for two FBMOCVD runs[a]

	M_a (g)	M_s (g)	T_s (°C)	T_b (°C)	Q_c (ml min^{-1})	Q_r (ml min^{-1})	t_d (h)	x
Rh/SiO_2	1	5	52	100	35	8.5	2.5	9×10^{-4}
Pd/SiO_2	0.6	2.5	45	60	86	0.8	3	5.7×10^{-3}

[a] Total pressure P = 50 Torr.

a mass M_a of the precursor complex is introduced as a powder into the sublimator, to which helical glass shells are added to obtain a better carrier gas/solid exchange area. A mass M_s of grains of support is poured into the column. The apparatus is placed under a reduced pressure of 0.1 Torr for 1 h whereas the bed temperature is maintained at 100 °C to remove water physisorbed on the support, the temperature of the sublimator being kept below 20 °C. Then the bed is heated to the temperature T_b and the pressure in the column is adjusted to the value P by introducing the carrier gas. The sublimator is plunged into a warm bath at temperature T_s and the gas flows (Q_c for the carrier gas and Q_r for the reactive gas) are adjusted. A dynamic vacuum is maintained to keep the pressure at the P value. The gas flow rate is chosen to maintain a bubbling fluidization regime in the column and to obtain a suitable molar ratio of precursor in the gas phase. Deposition begins, for a duration t_d. The molar ratio of sublimed precursor is x. At the end of the deposition, the temperature is slowly decreased to ambient. The vacuum and the gas flows are stopped and a slow air stream is passed through the apparatus until it reaches ambient pressure. The unsublimed precursor is recovered. The catalyst is removed from the column and used without any further treatment. For example, 1 wt% Rh/SiO_2 and 4.5 wt% Pd/SiO_2 catalysts were prepared using the parameters displayed in Table 4, starting from complexes $[Rh(\mu\text{-}Cl)(CO)_2$ and Pd(allyl)(Cp) respectively.

Several deposition studies were carried out on silica and alumina. Some results are shown on Table 5, where rhodium, palladium and platinum deposits have been selected. It is possible to attain very small aggregates with a high dispersion level. For instance, from $[Rh(\mu\text{-}Cl)(CO)_2]_2$ a 0.35 wt% rhodium deposit has been obtained; the particle size, measured by CO absorption, is near 1.1 nm and would correspond to a dispersion of more than 80% (calculated from CO absorption measurements as described in Ref. 35). Moreover, the initial

Table 5 Characterization of selected metal-supported catalysts obtained by FBMOCVD

Precursor complex	Metal (%)	Support	Average size of particles (nm)	Specific area ($m^2\ g^{-1}$)
$[Rh(\mu\text{-}Cl)(CO)_2]_2$	0.35	SiO_2	1.1	184[a]
$[Rh(\mu\text{-}Cl)(CO)_2]_2$	1.0	SiO_2	1.7	178[a]
$Rh(allyl)_3$	1.0	SiO_2	1.5	158[b]
Pd(allyl)(hfac)	1.2	Al_2O_3	2–100	130[c]
Pd(allyl)(Cp)	4.5	SiO_2	4.3	160[a]
$Pt(COD)(CH_3)_2$	2.3	SiO_2	3	175[a]

[a] Pure silica specific area is 170 $m^2\ g^{-1}$.
[b] Pure silica specific area is 150 $m^2\ g^{-1}$.
[c] Pure alumina specific area is 165 $m^2\ g^{-1}$.

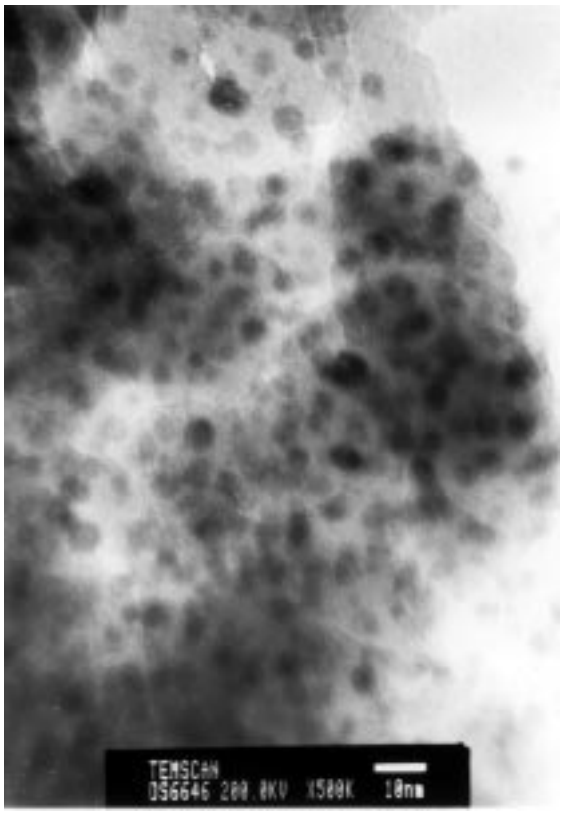

Figure 5 Transmission electron micrograph of a 4.5 wt% Pd/SiO_2 deposit produced from **5**.

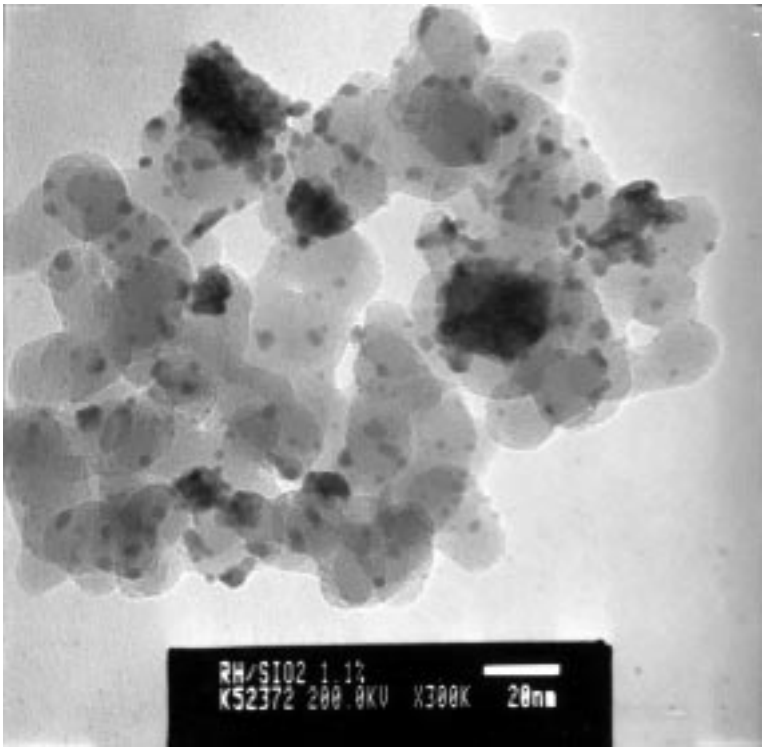

Figure 6 Transmission electron micrograph of a 1 wt% Rh/SiO_2 deposit produced from **1**.

specific area is not significantly modified as expected.

Two different rhodium complexes (**2** and **3**, Table 5) can give the same loading of metal and comparable values of particle size and dispersion (respectively 78% and 71%).

By fine-tuning the molar ratio of the complexes in the gas-phase, the size and the loading of the deposits can be controlled. Indeed, after an experiment using Pd(allyl)(Cp) when a high molar ratio of the precursor (Table 2, row 5) is fixed, the micrograph (see Fig. 5) shows mainly particles of 4.3 nm average size (Table 5, row 5) and a few larger aggregates of around 100 nm. In this case the loading of palladium reached 4.5 wt%. When a lower molar ratio is imposed (Table 2, row 2), 1 wt% Rh/SiO_2 deposits with 1.7 nm particles (Table 5, row 2) are produced from $[Rh(\mu\text{-}Cl)(CO)_2]_2$, as displayed in Fig. 6.

Similarly, platinum particles can be prepared from $Pt(COD)(CH_3)_2$. High-resolution microscopy revealed an average particle size of 3 nm with a remarkably homogeneous distribution on the support. No particles with sizes above 10 nm were noted.

In addition to the analyses of the metal content usually carried out by ICP, we checked the purity of the deposits by energy dispersion spectroscopy (EDS) on supported particles observed previously by transmission electron microscopy (TEM). The deposits present the same purities as the films prepared on planar substrates. For example, from $[Rh(\mu\text{-}Cl)(CO)_2]_2$ approx. 1.5% chlorine was detected, and from Pd(allyl)(hfac) no fluorine was found. Figure 7 displays the EDS analysis of palladium particles prepared from Pd(allyl)(hfac); no fluorine or carbon ($< 1\%$) was detected.

CATALYTIC TESTS

Several catalytic experiments were carried out on these supported materials, particularly on rhodium. Preliminary tests compared two catalysts, one prepared by the present process and one by a classical impregnation method, which starts from $RhCl_3 \cdot 3H_2O$ and involves successively a drying and a calcination step at 400 °C for 10 h and a reduction step under dihydrogen at 230 °C for 3 h. The catalyst prepared in this way was shown by

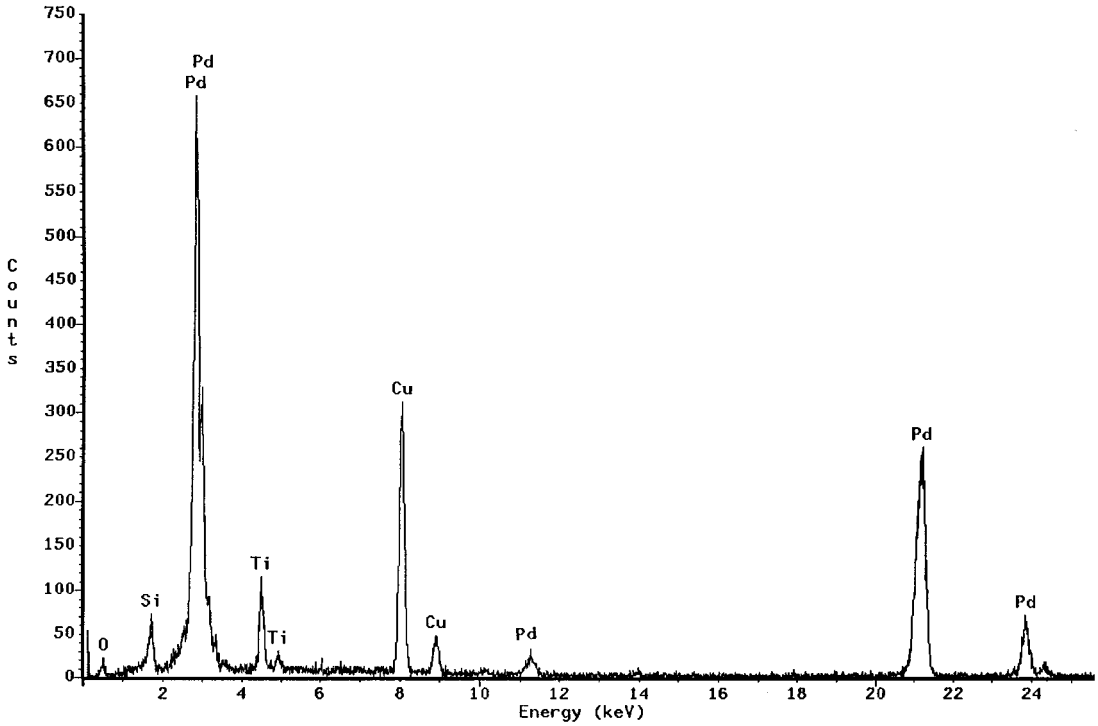

Figure 7 EDS spectrum of a palladium particle on SiO_2 obtained by Pd(allyl)(hfac) deposition at 45 °C in an H_2/He mixture (1 vol%). Titanium signals are due to the polar pieces of the microscope; copper signals arise from the grid support of the samples.

TEM EDS to contain rhodium particles of approx. 3 nm, the chlorine content being *ca* 8 wt%. Considering the two catalysts at 1% Rh/SiO_2, the FBMOCVD-prepared one displayed a 1190 h^{-1} activity for hydrogenation of 1-octene, against a 750 h^{-1} activity for the classical one at 1 bar H_2 and 25 °C. With FBMOCVD Rh/SiO_2 catalyst, activities of 140 h^{-1} for the hydrogenation of benzene to cyclohexane at 120 bar and 120 °C, and 28 h^{-1} for the hydrogenation of benzonitrile into benzylamine under the same conditions, were noted.

Rhodium-supported catalysts especially were examined for the hydrocarbonylation of methanol (200 bar, 200 °C). Various supports can be used, such as La_2O_3, SiO_2, Ce-doped SiO_2, Al_2O_3, activated carbon. The latter support gives a very good productivity of acetic acid, and higher acids [2.160 g (mg Rh)$^{-1}$], and the corresponding esters [0.04 g (mg Rh)$^{-1}$] and alcohols [0.012 g (mg Rh)$^{-1}$]. But the most interesting results were obtained for hydrocarbonylation of acetic acid to higher acids at 200 bar and 220 °C (6 h duration, 180 mmol CH_3COOH, 6.23 mmol HI, 2 wt% Rh/C*, 1.48×10^{-4} g-atoms of Rh): productivities of 1.8 g (g Rh)$^{-1}$ in propionic acid, 0.40 g (g Rh)$^{-1}$ in butanoic acids and 0.32 g (g Rh)$^{-1}$ in pentanoic acids have been obtained.[36]

Similarly the activities of the Pd/SiO_2 or Pd/Al_2O_3 catalysts were checked (0.0637 mol of 1-octene, 0.35 wt% Pd/SiO_2, 1.6×10^{-5} g-atoms of Pd). At 1 bar and 20 °C in ethanol, 1-octene is hydrogenated to octane with a 450 h^{-1} activity. Under the same conditions, 1.2% Pd/Al_2O_3 gives a 500 h^{-1} activity. Other catalytic reactions on palladium and platinum are under investigation.

CONCLUSION

FBMOCVD is a general method of preparing nano-sized metal aggregates homogeneously dispersed on high-specific-area substrates. The process requires metal-organic complexes having high vapor pressures. Under the conditions used here many different metals are accessible. The introduction of a suitable reactive gas allows ready removal of ligands, and under mild conditions highly pure deposits can be obtained. Similarly, various sup-

ports can be used, provided they can be fluidized. Preliminary results on alkene hydrogenation and alcohol hydrocarbonylation demonstrate the high activities of FBMOCVD-prepared catalytic materials.

Acknowledgments This work was supported by the European Economic Community through the BRITE–EURAM program, by the Conseil Scientifique de. l'Institut National Polytechnique (BQR Action) and by the Conseil Régional Midi-Pyrénées, which are gratefully acknowledged. J.-C.H. thanks the Ministère de l'Enseignement Supérieur et de la Recherche for his research grant. We are indebted to A. Reynes and Y. Caubel for help with the mass-spectrometry experiments and to J. Poujardieu for carrying out the TEM–EDS analyses at the Service de Microscopie Electronique en Transmission de l'Université Paul Sabatier de Toulouse. Thanks are due to J.-P. Guerlet, N. Petit and M. Malheiro for the loan of noble metals and for ICP analyses (Engelhard–CLAL, Paris), and to P. de Parseval (Service de Microsonde Electronique de l'Université Paul Sabatier de Toulouse) for characterization of the deposits. We are also grateful to our colleagues for helpful discussions: P. Tobaly (LIMHP, Villetaneuse), Professor A. Kiennemann and L. Chateau (EHICS, Strasbourg), Professor J.P. Couderc (ENSIGC, Toulouse), Professor J. Molinier, Professor R. Morancho and Dr F. Maury (ENSC, Toulouse).

REFERENCES

1. P. G. Harrison, *Nature (London)* **325**, 15 (1987).
2. A. Chauvel, G. Lefevre and L. Castex, *Procédés de Pétrochimie*, Institut Français du Pétrole, Editions Technip, Paris, 1985, and references therein.
3. B. Imelik, G. A. Martin and A. J. Renouprez, *Fundamental and Industrial Aspects of Catalysis by Metals*, CNRS, Paris, 1984.
4. K. Weissermel and H. J. Arpe, *Industrial Organic Chemistry*, VCH, Weinheim, 1993.
5. See for example: S. D. Jackson, J. Willis, G. D. McLellan, G. Webb, M. B. T. Keegan, R. B. Moyes, S. Simpson, P. B. Wells and R. Whymans, *J. Catal.* **139**, 191 (1993), and references therein.
6. M. Che and C. O. Benett, *Adv. Catal.* **36**, 55 (1985).
7. J. R. Anderson, *Structure of Metallic Catalysts*, Academic Press, London 1975.
8. J. A. Schwarz, *Chem. Rev.* **95**, 477 (1995).
9. See for example: B. Breitscheidel, J. Zieder and U. Schubert, *Chem. Mater*. **3**, 559 (1991), and references therein.
10. F. Figueras, S. Fuentes and C. Leclercq, *Growth and Properties of Metal Clusters*, Bourdon, J. (ed.) Elsevier (Netherlands) 1980, p525.
11. C. J. Brinker and G. W. Scherer, Sol–gel science In: *The Physics and Chemistry of Sol–Gel Processing*, Academic Press, New York, 1990.
12. Z. Duan and M. J. Hampden-Smith, *Chem. Mater*. **5**, 994 (1993).
13. E. C. Marboe, *US Patent*. 2 430 520, (1947).
14. M. J. Rand, *J. Electrochem. Soc.* **120**, 686 (1973).
15. M. J. Rand, *J. Electrochem. Soc.* **122**, 811 (1975).
16. J. E. Gozum, D. M. Pollina, J. A. Jensen and G. S. Girolami, *J. Am. Chem. Soc.* **110**, 2688 (1988).
17. Y. J. Chen, H. D. Kaesz, H. Thridandam and R. F. Hicks, *Appl. Phys. Lett.* **53**, 1591 (1988).
18. R. Kumar, M. Rashidi and R. J. Puddephatt, *Polyhedron* **8**, 551 (1989).
19. C. Dossi, A. Bartsch and P. Losi, *Adv. Synth. Methodol. Inorg. Chem*. 83 (1991).
20. C. Dossi, R. Psaro, R. Ugo, C. Z. Zhang and W. M. H. Sachtler, *J. Catal.* **149**, 92 (1994).
21. L. Sordelli, G. Martra, R. Psaro, C. Dossi and S. Coluccia, *J. Chem. Soc, Dalton Trans.* 720 (1996).
22. K. Omata, H. Mazaki, H. Yagita and K. Fujimoto, *Catal. Lett.* **4**, 123 (1990).
23. S. Köhler, S. Trautmann, H. Dropsch and M. Baerns, *Europacat-1* Montpellier France p 428 (1993).
24. F. Maury, *Chem. Vap. Deposition* **2**, 113 (1996).
25. R. U. Kirss, *Appl. Organometal. Chem.* **6**, 609 (1992).
26. P. Serp, R. Feurer, R. Morancho and P. Kalck, *J. Catal.* **157**, 294 (1995).
27. J. Powell and B. L. Shaw, *J. Chem. Soc. A* 583 (1968).
28. Y. S. Varshavskii and T. G. Cherkasova, *Russ. J. Inorg. Chem. Engl. Transl.* **12**, 899 (1967).
29. J.-C. Hierso, C. Satto, R. Feurer and P. Kalck, *Chem. Mater.* **3**, 2481 (1996).
30. Y. Tatsuno, T. Yoshida and S. Otsuka, *Inorg. Synth.* **19**, 220 (1979).
31. H. C. Clark and L. E. Manzer, *J. Organometal. Chem.* **59**, 411 (1973).
32. P. Serp, R. Feurer, R. Morancho, P. Kalck, J.-C. Daran and J. Vaissermann, *J. Organometal. Chem.* **498**, 41 (1995).
33. N. H. Dryden, R. V. Kumar, E. Ou, M. Rashidi, S. Roy, P. R. Norton and R. J. Puddephatt, *Chem. Mater.* **3**, 677 (1991).
34. B. Caussat, P. Serp, R. Rodriguez, R. Feurer, M. Hemati, P. Kalck and J.-P. Couderc, *"Recents Progrès en Génie des Procédés"* **9**, 38, p. 159 (1995), J. C. Charpentier (ed.) Lavvisier (Paris).
35. S. Boujana, D. Demry, J. Cressely, A. Kiennemann and J.-P. Hiendermann, *Catal. Lett.* **7**, 359 (1990).
36. P. Serp, L. Chateau, R. Feurer, A. Kiennemann and P. Kalck, *J. Mol. Catal*. submitted.

